

Hall effect in superconducting Fe(Se<sub>0.5</sub>Te<sub>0.5</sub>) thin filmsI. Tsukada,<sup>1,3,\*</sup> M. Hanawa,<sup>1,3</sup> Seiki Komiya,<sup>1,3</sup> T. Akiike,<sup>2,3</sup> R. Tanaka,<sup>2,3</sup> Y. Imai,<sup>2,3</sup> and A. Maeda<sup>2,3</sup><sup>1</sup>Central Research Institute of Electric Power Industry, 2-6-1 Nagasaka, Yokosuka, Kanagawa 240-0196, Japan<sup>2</sup>Department of Basic Science, The University of Tokyo, 3-8-1 Komaba, Meguro-ku, Tokyo 153-8902, Japan<sup>3</sup>JST, TRIP, Sanbancho, Chiyoda-ku, Tokyo 102-0075, Japan

(Received 28 October 2009; revised manuscript received 5 January 2010; published 22 February 2010; corrected 8 March 2010)

The Hall effect is investigated for eight superconducting Fe(Se<sub>0.5</sub>Te<sub>0.5</sub>) thin films grown on MgO and LaSrAlO<sub>4</sub> substrates with different transition temperatures ( $T_c$ ). The normal Hall coefficients ( $R_H$ ) have positive values with magnitude of  $1 \sim 1.5 \times 10^{-3}$  cm<sup>3</sup>/C at room temperature for the all samples. With decreasing temperature, we find two characteristic types of behavior in  $R_H(T)$  depending on  $T_c$ . For thin films with lower  $T_c$  (typically  $T_c < 5$  K),  $R_H$  start decreasing approximately below  $T = 250$  K toward a negative side, some of which shows sign reversal at  $T = 50 \sim 60$  K, but turns positive toward  $T = 0$  K. On the other hand, for the films with higher  $T_c$  (typically  $T_c > 9$  K),  $R_H$  leaves almost unchanged down to  $T \approx 100$  K, and then starts decreasing toward a negative side. Around the temperatures when  $R_H$  changes its sign from positive to negative, obvious nonlinearity is observed in the field-dependence of Hall resistance as to keep the low-field  $R_H$  positive while the high-field  $R_H$  negative. Thus, the electronic state just above  $T_c$  is characterized by  $n_e$  (electron density)  $> n_h$  (hole density) with keeping  $\mu_e < \mu_h$ . These results suggest the dominance of electron density to the hole density is an essential factor for the occurrence of superconductivity in Fe-chalcogenide superconductors.

DOI: [10.1103/PhysRevB.81.054515](https://doi.org/10.1103/PhysRevB.81.054515)

PACS number(s): 74.78.-w, 74.25.F-, 74.62.Dh, 74.70.Dd

The discovery of superconductivity in iron oxypnictides<sup>1</sup> opened routes for exploration of high-temperature (high- $T_c$ ) superconductors other than cuprates. Triggered by the discovery of LaFeAs(O<sub>1-x</sub>F<sub>x</sub>),<sup>1</sup> a tremendous number of studies were very quickly undertaken on these materials. The presence of superconductivity in Fe-based binary compounds, FeSe,<sup>2,3</sup> is surprising, because the  $T_c$  of a FeSe system exceeds 36 K under high pressure despite its simple crystal structure,<sup>4</sup> which is comparable to MgB<sub>2</sub>, another binary compound superconductor. Interestingly, FeSe had already been investigated in detail, but for its properties as a ferromagnetic semiconductors. According to the first investigation by Feng *et al.*,<sup>5</sup> and by several other related works,<sup>6-8</sup> the transport properties of FeSe have been summarized in the following four characteristic features. First, a majority of the charge carriers at room temperature are holes, and the resistivity decreases with increasing hole concentrations. Second, spontaneous magnetization is present at room temperatures. Third, band calculations suggest the coexistence of hole- and electron-type carriers at room temperature. Finally, sign reversal of the Hall coefficient  $R_H$  occurs below 100 K when the material is doped sufficiently with holes. However, the relationship between these normal-state electronic properties and the superconducting properties of these materials has not yet been clarified.

One of the features that make Fe-based superconductors exotic is its paring symmetry as was first proposed for LaFeAs(O<sub>1-x</sub>F<sub>x</sub>) by Mazin *et al.*,<sup>9</sup> and Kuroki *et al.*,<sup>10</sup> which requires  $(\pi, \pi)$  nesting of the Fermi surface. However, for the FeSe system, it remains a point of argument whether  $(\pi, \pi)$  nesting<sup>11,12</sup> or another  $(\pi, 0)$  nesting<sup>13</sup> is responsible for the formation of Cooper pairs. This controversy gathers our attention and leads us to an important question whether the Fe-pnictides and Fe-chalcogenide is essentially the same superconductor, or not. To resolve this it is important to quantitatively investigate the electronic transport properties

in the relation to the superconductivity. Recently, we succeeded in growing superconducting Fe(Se<sub>0.5</sub>Te<sub>0.5</sub>) thin films on MgO and LaSrAlO<sub>4</sub> (LSAO) substrates,<sup>14</sup> in which we found that a choice of substrates was crucial for the growth of Fe(Se,Te) films. The strong substrates dependence has been also discussed with respect to an epitaxial strain in previous works on FeSe and Fe(Se,Te) thin films.<sup>15-21</sup> In this paper, we report the results of detailed Hall-effect measurements on several Fe(Se<sub>0.5</sub>Te<sub>0.5</sub>) thin films with different  $T_c$ 's, conducted in order to obtain deeper insight into the electronic states of this material, and to investigate potential routes toward a higher  $T_c$ . We confirm the coexistence of electrons and holes first, and, in addition, we find (1) that there is an intimate relation between the temperature dependence of  $R_H$  and  $T_c$ , and (2) that the electronic state just above  $T_c$  is characterized by  $n_e$  (electron density)  $> n_h$  (hole density) with keeping  $\mu_e < \mu_h$ .

Fe(Se<sub>0.5</sub>Te<sub>0.5</sub>) films highly oriented along the  $c$  axis were grown by pulsed-laser deposition (PLD) as described elsewhere.<sup>14</sup> We prepared eight thin-film samples for the Hall-effect measurements. Detailed specifications of the films are summarized in Table I. Six films were prepared from a stoichiometric FeSe<sub>0.5</sub>Te<sub>0.5</sub> sintered target, and two were prepared from a FeSe<sub>0.5</sub>Te<sub>0.75</sub> target containing excess Te. We prepared two films simultaneously during each deposition, one on MgO(100) and the other on LaSrAlO<sub>4</sub>(001) in order to purely extract the substrate dependence. Samples A and D, B and E, C and F, and G and H were each grown in the same deposition process. All of the films were deposited in a six-terminal shape using a metal mask appropriate for both resistivity and Hall-effect measurements. The crystal structure was investigated by an ordinary  $\theta$ - $2\theta$  x-ray diffraction. Thicknesses of the films were estimated by Dektak 6M stylus profiler. Resistivity and Hall-effect measurements were obtained using PPMS for temperatures down to  $T = 2$  K.

TABLE I. Specifications of the  $\text{Fe}(\text{Se}_{1-x}\text{Te}_x)$  films.

| Name     | Substrate               | Target                              | $T_c$<br>(K) | Thickness<br>(nm) | $c$ -axis length<br>(Å) | Se/Te ratio |
|----------|-------------------------|-------------------------------------|--------------|-------------------|-------------------------|-------------|
| Sample A | MgO(100)                | $\text{FeSe}_{0.5}\text{Te}_{0.5}$  | 9.2          | 55                | 5.92                    | 0.668/0.332 |
| Sample B | MgO(100)                | $\text{FeSe}_{0.5}\text{Te}_{0.5}$  | 8.8          | 164               | 5.90                    |             |
| Sample C | MgO(100)                | $\text{FeSe}_{0.5}\text{Te}_{0.5}$  | 4.6          | 135               | 5.86                    |             |
| Sample D | $\text{LaSrAlO}_4(001)$ | $\text{FeSe}_{0.5}\text{Te}_{0.5}$  | $<2$         | 80                | 5.79                    | 0.666/0.334 |
| Sample E | $\text{LaSrAlO}_4(001)$ | $\text{FeSe}_{0.5}\text{Te}_{0.5}$  | 2.0          | 250               | 5.88                    |             |
| Sample F | $\text{LaSrAlO}_4(001)$ | $\text{FeSe}_{0.5}\text{Te}_{0.5}$  | $<2$         | 190               | 5.84                    |             |
| Sample G | MgO(100)                | $\text{FeSe}_{0.5}\text{Te}_{0.75}$ | 9.4          | 212               | 5.93                    | 0.588/0.412 |
| Sample H | $\text{LaSrAlO}_4(001)$ | $\text{FeSe}_{0.5}\text{Te}_{0.75}$ | 3.4          | 348               | 5.90                    | 0.552/0.448 |

All the films shown in this paper have a highly  $c$ -axis oriented structure in common, while their  $c$ -axis length is a little bit scattered. As was shown in our previous paper<sup>14</sup> and is summarized again in Table I, the  $c$ -axis length of the prepared films spreads out from 5.79 to 5.93 Å, which are shorter than that reported for polycrystalline samples.<sup>22</sup> Thus, we suspected that the chemical composition of the films was deviated largely from that of the target, and carried out an EDX measurement to the selected films. The obtained results of Se/Te ratio is shown in Table I for samples A, D, G, and H. The Se content is richer than that of Te in common, which is probably the main reason for the observed short  $c$ -axis lengths. This tendency is also consistent with the fact that we obtain the films with more Te content when using the  $\text{FeSe}_{0.50}\text{Te}_{0.75}$  target (compare samples A and G, for example). Such a deviation of the chemical composition between targets and films is probably due to the difference of the vapor pressure of Se and Te, which become crucial in the thin-film growth process using high-vacuum conditions like our PLD method. However, it should be also emphasized that the Se/Te ratio is not different much between the films prepared at the same time (compare samples A and D, for example). This means that the observed differences between the films on MgO and those on  $\text{LaSrAlO}_4$  substrates are not caused by the difference of the Se/Te ratio, but rather by the difference of substrate materials. A more comprehensive investigation of the crystalline structure using four-circle x-ray diffractometer and transmission electron microscopy (TEM) is necessary for revealing how the substrate gives influence to  $\text{Fe}(\text{Se}_{0.5}\text{Te}_{0.5})$  on it.

Figure 1 shows the temperature dependence of the resistivity for the eight samples. The resistivity at room temperatures are spread only within 450 and 700 mΩ cm, which is sufficiently low for metallic (and superconducting) behavior. However, we find that  $\rho(T)$  may be classified into three groups from the measurements down to  $T=2$  K. Figure 1(a) represents the most metallic group (samples A and G), which exhibits crossover from semiconducting ( $d\rho/dT < 0$ ) to metallic ( $d\rho/dT > 0$ ) behavior with decreasing temperature.  $T_c$  exceeds 9 K, which is the highest such value among all the films. The second group represents an “intermediate” group (samples B, C, D, and H) and is illustrated in Fig. 1(b). This group is also characterized by  $d\rho/dT > 0$  at intermediate temperatures, but the slope turns again to  $d\rho/dT < 0$  before

the transition to superconductivity. The samples in this group also exhibit lower  $T_c$  than those in the first group. The third group (samples E and F) is the most insulating group [Fig.

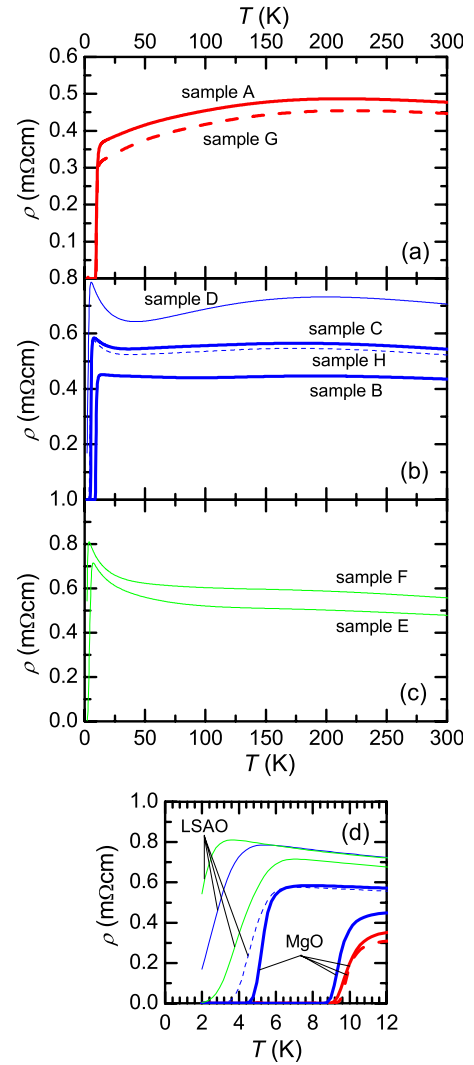


FIG. 1. (Color online) Temperature dependence of resistivity of (a) samples A and G (red line), (b) samples B, C, D, and H (blue line), and (c) samples E and F (green line). Thick and thin lines are for the films grown on MgO and  $\text{LaSrAlO}_4$ , respectively. (d)  $\rho(T)$  around  $T_c$  regions.

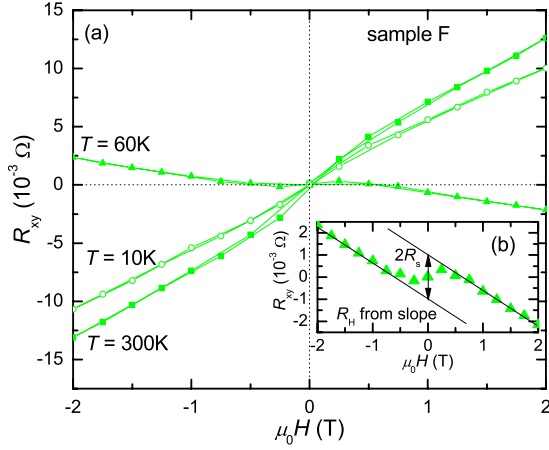


FIG. 2. (Color online) (a) Hall resistance ( $R_{xy}$ ) of sample F measured by sweeping field as  $\mu_0 H = 0 \rightarrow 2 \rightarrow -2 \rightarrow 0$  T taken at  $T = 300, 60$ , and  $10$  K. (b) The close-up figure of  $T = 60$  K data.

1(c)], as it never exhibits metallic ( $d\rho/dT > 0$ ) behavior. As shown in Fig. 1(d), all the films become superconducting even though this state is not observed for  $T \geq 2$  K for samples D and F.

For the evaluation of  $R_H$ , we first need to measure transverse resistance  $R_{xy}$  by sweeping the magnetic field, because the presence of the anomalous Hall effect (AHE) (Ref. 23) has already been reported for FeSe by Feng *et al.*<sup>5</sup> An example of the typical behavior is shown for sample F in Fig. 2(a). We sweep the magnetic field from  $\mu_0 H = 0 \rightarrow 2 \rightarrow -2 \rightarrow 0$  T, and observed that  $R_{xy}$  showed a steplike behavior around the  $H = 0$  T indicating a contribution from the AHE. Thus, it is likely that the present Fe(Se<sub>0.5</sub>Te<sub>0.5</sub>) thin films has spontaneous magnetization, although we cannot measure the magnetization due to the insufficient sample volume.  $R_{xy}$  is expressed as the sum of a normal Hall term ( $R_H B$ ) and an anomalous Hall term ( $R_s \mu_0 M$ ). A steep increase in  $R_{xy}$  is only observed between  $-0.5 \text{ T} < \mu_0 H < 0.5 \text{ T}$  [Fig. 2(b)], so we reasonably determine  $R_H$  by linearly fitting of  $R_{xy}$  vs  $\mu_0 H$  between  $-2 \text{ T} < \mu_0 H < -1 \text{ T}$ . Figure 2(a) also shows that  $R_H > 0$  at  $T = 300$  K, that  $R_H < 0$  at  $T = 60$  K, and that  $R_H > 0$  at  $T = 10$  K. It should be noted that the sign of  $R_s$  is not influenced by the sign reversals of  $R_H$ . Although we do not further discuss the detailed  $T$  dependence of  $R_s$  in this paper,  $R_s$  appears roughly proportional to  $\rho(T)$  and/or  $\rho^2(T)$ , which is consistent with conventional scenarios of skew scattering effect and/or side jump effects.<sup>24</sup>

After removing the contribution associated with AHE, we plot  $R_H$  in the weak-field limit for all samples as shown in Fig. 3.  $R_H$  is almost independent of  $T$  around room temperature, and has a value between  $1 \sim 1.5 \times 10^{-3} \text{ cm}^3/\text{C}$ . This is consistent with the value reported by Feng and co-workers,<sup>5,6</sup> but it is half of the value reported by Wu *et al.*<sup>15</sup> The most metallic group of the samples maintains a nearly constant  $R_H$  down to 100 K. Below this temperature,  $R_H$  starts decreasing. We observe sign reversal only once for both samples A and G. It is surprising that these samples show almost identical  $R_H(T)$  and also  $\rho(T)$ , even though they were prepared from different targets. This suggests the existence of a close correlation between  $\rho$  and  $R_H$ . The  $T$  dependence observed here

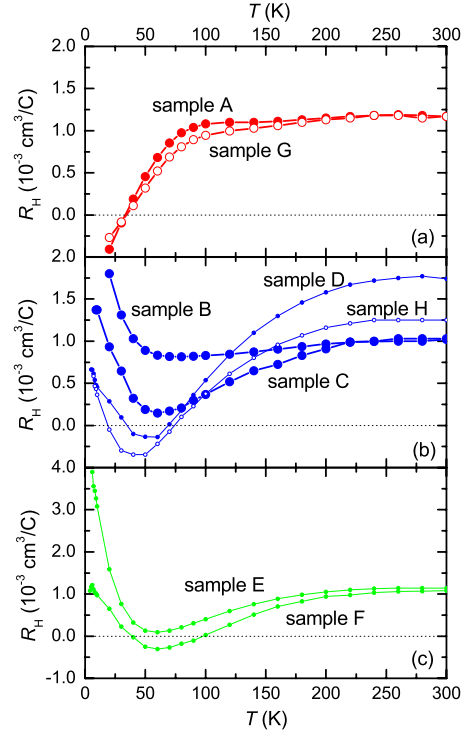


FIG. 3. (Color online) Temperature dependence of weak-field normal Hall coefficients of Fe(Se<sub>0.5</sub>Te<sub>0.5</sub>) thin films of (a) samples A and G (red line), (b) samples B, C, D, and H (blue line), and (c) samples E and F (green line). Thick and thin lines are for the film grown on MgO and LaSrAlO<sub>4</sub>, respectively.

is similar to that observed for Fe(Se<sub>0.5</sub>Te<sub>0.5</sub>) thin films by Wu *et al.*,<sup>15</sup> in which the author claimed that the sign reversal is strong evidence of the multiband nature of the band structure. Figures 3(b) and 3(c) show the  $R_H$  value of the samples belonging to the second and the third groups, as a function of temperature. These  $R_H$  values typically become more positive at low temperatures. This suggests that the normal-state transport properties for  $T \gtrsim T_c$  are dominated by holetype conduction, which is a clear contrast to the behavior observed in samples A and G.

The temperature-dependent results suggest a finite correlation between the localization behavior of  $\rho(T)$  and the upturn in  $R_H$ . The samples with  $T_c$  less than 5 K exhibit a gradual decrease of  $R_H$  with decreasing temperature starting from  $T = 250$  K.  $R_H$  decreases continuously until a temperature of 60 K is reached, it attains its minimum regardless of its sign being positive or negative, and finally turns increasing again to the positive side toward  $T_c$ . The upturn in  $R_H$  toward  $T = 0$  K is observed in samples C, D, E, F, and H while neither samples A nor G show such increase, which may allow us to relate the presence of this upturn to relatively low  $T_c$ . However, it should be noted that such an upturn toward  $T_c$  is also observed in sample B that shows  $T_c = 8.8$  K as high as that of samples A and G, and we cannot say that  $R_H(T)$  behavior at  $T \gtrsim T_c$  and its sign just above  $T_c$  is not directly related to  $T_c$ . Instead, we can find more robust correlation between  $R_H$  and  $T_c$ . Let us see  $R_H(T)$  of sample B again. Despite a strong upturn of  $R_H$  in sample B below

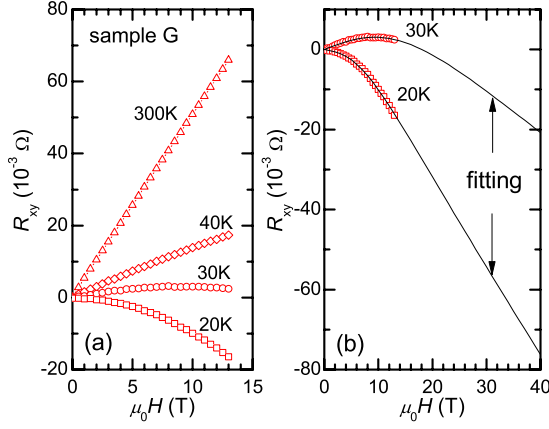


FIG. 4. (Color online) (a) High-field  $R_{xy}$  of sample G at  $T = 300, 40, 30$ , and  $20$  K. The nonlinearity to  $H$  becomes enhanced at  $T = 30$  and  $20$  K as a signature of coexistence of  $p$ - and  $n$ -type carriers. (b) Fitting with Eq. (1) to the  $T = 30$  K and  $20$  K data.

60 K,  $R_H$  looks almost independent of temperature between  $100 \text{ K} < T < 250 \text{ K}$  similar to that observed in samples A and G. Thus, we should conclude that a strong correlation exists between  $T_c$  and the  $T$  dependence of  $R_H$  below  $250 \text{ K}$ .

In order to further explore the normal-state transport properties of FeSe system, we need to explicitly treat the motion of electron- and hole-type carriers. Fortunately, there are several band calculations in the literature for the FeSe system, and based on these, it has been accepted that, at least, four bands which originate from different Fe  $3d$  orbital cross the Fermi level.<sup>11,12</sup> Two of these contribute hole-type conduction, and the other two contribute electron-type conduction. To minimize complexity, we do not consider all four of these bands, at once. Instead, we apply a simplified two-carrier model including one electron band (with electron density  $n_e$  and mobility  $\mu_e$ ) and one hole-type band (with hole density  $n_h$  and mobility  $\mu_h$ ), and from this try to extract phenomenological but essential behavior of  $R_H(T)$ . Since we do not know a mathematical expression of  $R_H$  suitable for two-dimensional cylindrical Fermi surfaces, we borrow a classical expression for the Hall coefficient of three-dimensional isotropic semiconductors in the presence of both electron- and hole-type carriers:<sup>25</sup>

$$R_H = \frac{1}{e} \frac{(n_h - n_e b^2) + b^2 \mu_h^2 B^2 (n_h - n_e)}{(b n_e + n_h)^2 + b^2 \mu_h^2 B^2 (n_h - n_e)^2}, \quad (1)$$

where  $b = \mu_e / \mu_h$ , and  $B$  is a magnetic flux density. This equation predicts immediately a nonlinear dependence of  $R_{xy}$  ( $= R_H B$ ) on applied field, which can be observed at field of several Tesla depending on the coefficients in the equation.

The fitting of  $R_{xy}$  is most successfully performed for sample G. To see how the sign change occurs in  $R_H$ , we plot  $R_{xy}$  by sweeping the field up to  $\mu_0 H = 13 \text{ T}$  [Fig. 4(a)]. Equation (1) predicts that  $R_H = e^{-1} \cdot (n_h \mu_h^2 - n_e \mu_e^2) / (n_e \mu_e + n_h \mu_h)^2$  in the limit of  $B = 0$ , while  $R_H = e^{-1} \times 1 / (n_h - n_e)$  in the limit of  $B = \infty$ . At  $T = 300 \text{ K}$ ,  $R_H$  looks almost linear in  $H$ , indicating the hole-type transport is dominant. Furthermore, it is likely

that hole-type transport is dominant even at  $T = 40 \text{ K}$ . At  $T = 30 \text{ K}$  and  $20 \text{ K}$ , on the other hand, obvious nonlinear behavior is observed. We successfully fit both data with Eq. (1), as shown by the solid lines in Fig. 4(b), and obtain  $n_e - n_h = 3.38 \times 10^{22} \text{ cm}^{-3}$  at  $T = 30 \text{ K}$  and  $n_e - n_h = 1.44 \times 10^{22} \text{ cm}^{-3}$  at  $T = 20 \text{ K}$ . Although the values themselves are strongly dependent on the particular model that we used, in any case the density of electron-type carriers rapidly increases with  $T$  decreasing from higher temperature, and this density exceeds that of hole-type carriers before superconducting transition. The data at  $T = 30 \text{ K}$  is most notable, because the slope at high field is negative while that at low field is positive, which means  $p\mu_h^2 - n\mu_e^2 > 0$  and  $n_h - n_e < 0$ . This gives the relation that  $\mu_h > \mu_e$ , which is consistent with a result previously indicated in the literature.<sup>6</sup>

Let us first compare the present results to the reported Hall effect measured for single crystals. The normal-state Hall coefficients have been already reported for  $\text{Ba}(\text{Fe}_{2-x}\text{Co}_x\text{As}_2)$  and  $\text{Ba}(\text{Fe}_2\text{As}_{2-x}\text{P}_x)$  single crystals.<sup>26-28</sup> They commonly exhibit negative  $R_H$  at room temperatures for  $x = 0$ , which is explained as that the electron mobility dominates the hole mobility. The present results for  $\text{Fe}(\text{Se}_{0.5}\text{Te}_{0.5})$  show a clear contrast to  $\text{Ba}(\text{Fe}_2\text{As}_2)$ ;  $R_H$  shows a positive value exceeding  $1 \times 10^{-3} \text{ cm}^3/\text{C}$  for the eight samples. By taking the fact that such positive  $R_H$  has been observed for Te-free FeSe thin films<sup>5</sup> and for Se-free FeTe thin films<sup>29</sup> into account, it is likely that  $\text{Fe}(\text{Se}_{1-x}\text{Te}_x)$  has a positive  $R_H$  at any  $x$  ( $0 \leq x \leq 1$ ), which is probably one of the essential differences to distinguish FeSe-based superconductors from FeAs-based one. We may consider two possible origins of the difference. One is that the number of outer electrons is different between pnictogen and chalcogen, and the other is more specific reasons, such as band structures. Actually our result indicates that the hole mobility is larger than the electron mobility, while the opposite relation is deduced for  $\text{Ba}(\text{Fe}_{2-x}\text{Co}_x\text{As}_2)$ ,<sup>26,27</sup> which can be attributed to the details and local features of the electronic band structure.

Next, we discuss how to understand the observed variation of  $T_c$  and the Hall coefficients in the context of reported theories. One of the anomalous features of Fe-based superconductors is their pairing symmetry.<sup>10</sup> A likely symmetry is  $s_{\pm}$  wave, which requires a finite nesting condition between electron- and hole-type bands centered at the  $M$  and  $\Gamma$  points in a reciprocal space, respectively. Singh *et al.* discussed how this nesting condition is influenced by carrier doping.<sup>30</sup> They pointed out that spin density wave (SDW) instability becomes dominant over superconductivity when the nesting is too good, and with electron doping (shrinkage of the hole-type Fermi surface), the nesting condition becomes worse and superconductivity results. Our findings would be consistent with this scenario if the films with higher  $T_c$  had smaller hole-type Fermi surfaces than the lower- $T_c$  films, and they do appear this way. The gradual decrease of  $R_H$  below  $T = 250 \text{ K}$  and the associated increase of  $R_H$  at  $T \gtrsim T_c$  for films with lower  $T_c$  indicate the dominance of hole-type carriers throughout the whole temperature range. The dependence of



$R_H$  on  $T$  may be due to the different  $T$  dependences of  $\mu_h$  and  $\mu_e$ . On the other hand, the higher- $T_c$  films exhibit a drastic change from hole- to electron-type transport, which strongly indicates that the Fermi level of the higher- $T_c$  films is located above that of the lower- $T_c$  films around  $T \gtrsim T_c$ . Thus, one possible reason why sample G has a higher  $T_c$  is the shrinkage of the hole-type Fermi surface. Experimentally, we confirm that the magnitude of the resistivity in the normal-state scales well with the  $c$ -axis length of the films.<sup>14</sup> Therefore, we infer that the short  $c$ -axis length and associated lattice deformations sensitively change the position of the Fermi level in Fe(Se<sub>0.5</sub>Te<sub>0.5</sub>) thin films, and that we are able to detect this shift using Hall-effect measurements. To confirm this inference, we need to carry out more comprehensive measurements of the Hall effect in FeSe systems as a function of doping and crystal structure.

In conclusion, we measure the temperature dependence of the normal Hall coefficients, which is positive in contrast to Ba(Fe<sub>2</sub>As<sub>2</sub>), for several Fe(Se<sub>0.5</sub>Te<sub>0.5</sub>) thin films and find a

strong correlation between  $R_H(T)$  and  $T_c$ .  $R_H(T)$  of the most metallic samples remains almost constant down to  $T=100$  K, and then start decreasing toward negative side, which is driven by the change in the population of electron- and hole-type carriers, and the charge transport at temperatures just above  $T_c$  is dominated by electron-type carriers. On the other hand, in more insulating samples, the dominant carriers remain hole-type, and the  $R_H$  exhibits a different temperature dependence. We proposed the analysis of non-linear Hall resistivity, which can be the entrance to decompose the role of carrier concentrations and mobilities on the electronic structure and superconductivity in the iron-chalcogenide superconductors.

We thank T. Kawaguchi, H. Ikuta, A. Ichinose, J. Shimoyama, and K. Kishio for fruitful discussions and for sharing the unpublished data. We also thank H. Kontani and K. Ohgushi for valuable discussions.

\*ichiro@criepi.denken.or.jp

- <sup>1</sup>Y. Kamihara, T. Watanabe, M. Hirano, and H. Hosono, *J. Am. Chem. Soc.* **130**, 3296 (2008).
- <sup>2</sup>F. C. Hsu, J. Y. Luo, K. W. Yeh, T. K. Chen, T. W. Huang, P. M. Wu, Y. C. Lee, Y. L. Huang, Y. Y. Chu, D. C. Yan, and M. K. Wu, *Proc. Natl. Acad. Sci. U.S.A.* **105**, 14262 (2008).
- <sup>3</sup>Y. Mizuguchi, F. Tomioka, S. Tsuda, T. Yamaguchi, and Y. Takanaka, *Appl. Phys. Lett.* **94**, 012503 (2009).
- <sup>4</sup>S. Medvedev, T. M. McQueen, I. A. Troyan, T. Palasyuk, M. I. Eremets, R. J. Cava, S. Naghavi, F. Casper, V. Ksenofontov, G. Wortmann, and C. Felser, *Nature Mater.* **8**, 630 (2009).
- <sup>5</sup>Q. J. Feng, D. Z. Shen, Y. J. Zhang, B. S. Li, B. H. Li, Y. M. Lu, X. W. Fan, and H. W. Liang, *Appl. Phys. Lett.* **88**, 012505 (2006).
- <sup>6</sup>X. J. Wu, D. Z. Shen, Z. Z. Zhang, J. Y. Zhang, K. W. Liu, B. H. Li, Y. M. Lu, B. Yao, B. S. Li, C. X. Shan, X. W. Fan, H. J. Liu, and C. L. Yang, *Appl. Phys. Lett.* **90**, 112105 (2007).
- <sup>7</sup>K. W. Liu, J. Y. Zhang, D. Z. Shen, C. X. Shan, B. H. Li, Y. M. Lu, and X. W. Fan, *Appl. Phys. Lett.* **90**, 262503 (2007).
- <sup>8</sup>X. J. Wu, Z. Z. Zhang, J. Y. Zhang, B. H. Li, Z. G. Ju, Y. M. Lu, B. S. Li, and D. Z. Shen, *J. Appl. Phys.* **103**, 113501 (2008).
- <sup>9</sup>I. I. Mazin, D. J. Singh, M. D. Johannes, and M. H. Du, *Phys. Rev. Lett.* **101**, 057003 (2008).
- <sup>10</sup>K. Kuroki, S. Onari, R. Arita, H. Usui, Y. Tanaka, H. Kontani, and H. Aoki, *Phys. Rev. Lett.* **101**, 087004 (2008).
- <sup>11</sup>A. Subedi, L. Zhang, D. J. Singh, and M. H. Du, *Phys. Rev. B* **78**, 134514 (2008).
- <sup>12</sup>Y. Xia, D. Qian, L. Wray, D. Hsieh, G. F. Chen, J. L. Luo, N. L. Wang, and M. Z. Hasan, *Phys. Rev. Lett.* **103**, 037002 (2009).
- <sup>13</sup>M. J. Han and S. Y. Savrasov, *Phys. Rev. Lett.* **103**, 067001 (2009).
- <sup>14</sup>Y. Imai, R. Tanaka, T. Akiike, M. Hanawa, I. Tsukada, and A. Maeda, *Jpn. J. Appl. Phys.* (to be published).
- <sup>15</sup>M. K. Wu, F. C. Hsu, K. W. Yeh, T. W. Huang, J. Y. Luo, M. J. Wang, H. H. Chang, T. K. Chen, S. M. Rao, B. H. Mok, C. L. Chen, Y. L. Huang, C. T. Ke, P. M. Wu, A. M. Chang, C. T. Wu, and Y. P. Perng, *Physica C* **469**, 340 (2009).
- <sup>16</sup>T. G. Kumary, D. K. Baisnab, J. Janaki, A. Mani, R. M. Sarguna, P. K. Ajikumar, A. K. Tyagi, and A. Bharathi, *Superconduct. Sci. Technol.* **22**, 095018 (2009).
- <sup>17</sup>M. Wang, J. Luo, T. Huang, H. Chang, T. Chen, F. Hsu, C. Wu, P. Wu, A. Chang, and M. Wu, arXiv:0904.1858 (unpublished).
- <sup>18</sup>Y. F. Nie, E. Brahimi, J. I. Budnick, W. A. Hines, M. Jain, and B. O. Well, *Appl. Phys. Lett.* **94**, 242505 (2009).
- <sup>19</sup>Y. Han, W. Y. Li, L. X. Cao, S. Zhang, B. Zu, and B. R. Zhao, *J. Phys.: Condens. Matter* **21**, 235702 (2009).
- <sup>20</sup>E. Bellingeri, R. Buzio, A. Gerbi, D. Marre', S. Congiu, M. Cimberle, M. Tropeano, A. Siri, A. Palenzona, and C. Ferdeghini, *Superconduct. Sci. Technol.* **22**, 105007 (2009).
- <sup>21</sup>W. Si, Z.-H. Lin, Q. Jie, W.-G. Yin, J. Zhou, G. Gu, P. D. Johnson, and Q. Li, *Appl. Phys. Lett.* **95**, 052504 (2009).
- <sup>22</sup>M. H. Fang, H. M. Pham, B. Qian, T. J. Liu, E. K. Vehstedt, Y. Liu, L. Spinu, and Z. Q. Mao, *Phys. Rev. B* **78**, 224503 (2008).
- <sup>23</sup>Anomalous Hall effect is classified in two groups from its mechanism; one has an internal mechanism originated from multiband effect and spin-orbit coupling discussed by Karplus and Luttinger, while the other has an external mechanism such as an skew scattering or side jump mechanisms investigated by Smit and Berger. In this paper, we refer to the latter one as AHE following to the previous research by Feng *et al.*, which report the presence of spontaneous magnetization in FeSe thin films.
- <sup>24</sup>See, for example, *The Hall Effect and Its Applications*, edited by C. L. Chien and C. R. Westgate (Plenum Press, New York, 1980).
- <sup>25</sup>See, for example, *Semiconductors*, edited by R. A. Smith (Cambridge University Press, Cambridge, England, 1978).
- <sup>26</sup>F. Rullier-Albenque, D. Colson, A. Forget, and H. Alloul, *Phys. Rev. Lett.* **103**, 057001 (2009).
- <sup>27</sup>L. Fang, H. Luo, P. Cheng, Z. Wang, Y. Jia, G. Mu, B. Shen, I. I. Mazin, L. Shan, C. Ren, and H. H. Wen, *Phys. Rev. B* **80**,

- 140508(R) (2009).
- <sup>28</sup>S. Kasahara, T. Shibauchi, K. Hashimoto, K. Ikada, S. Tonegawa, R. Okazaki, H. Ikeda, H. Takeya, K. Hirata, T. Terashima, and Y. Matsuda, arXiv:0905.4427v3 (unpublished).
- <sup>29</sup>Y. Han, W. Y. Li, L. X. Cao, X. Y. Wang, B. Xu, B. R. Zhao, Y. Q. Guo, and J. L. Yang, Phys. Rev. Lett. **104**, 017003 (2010).
- <sup>30</sup>D. J. Singh, M. H. Du, L. Zhang, A. Subedi, and J. An, Physica C **469**, 886 (2009).